Published in Photonics Technology Letters (IEEE) 10, issue 10, 1371-1373, 1998
which should be used for any reference to this work

Multiwavelength Light Emitters for Scanning Applications Fabricated by Flipchip Bonding

D. Hofstetter, D. Sun, C. Dunnrowicz, M. Kneissl, and D. W. Treat

Abstract—**We present a multiwavelength light source which was fabricated using a self-aligned flipchip bonding technique. The device consists of an InGaN–GaN light-emitting diode emitting light at around 420 nm, on top of which we flipchip-bonded a monolithically integrated red/infrared dual-beam laser. The upper two lasers were built by selective removal of the red laser, and subsequent regrowth of an infrared laser structure. Since all processes, including the deposition of the PbSn solder bumps for bonding, were based on photolithographic precision, tight alignment tolerances of ±2 μm in the lateral direction could be fulfilled between the ridge waveguides of the three light emitters. For a high-speed color scanning system, this is an important design criterion because it will allow the use of a single scanning optics for the three laser beams.**

Index Terms— **Flipchip-bonding, hybrid integration, lateral alignment, multiwavelength light emitters.**

I. Introduction

FOR A NUMBER of scanning applications, the use of multiple laser beams with different emission wavelengths is an important technology. Ideally, these light emitters would be integrated on a single substrate, either combined monolithically or in a hybrid way. However, since the required wavelength differences between them might span a wide range, monolithic integration is not always feasible. A variety of possibilities, among them monolithic solutions using intermixing [1], stacked growth [2], wafer fusion [3], and side-by-side etch and regrowth [4], or hybrid integration schemes such as side-by-side mounting have already been investigated for achieving multiple wavelength lasers.

In this letter, we report a prototype of a triple-wavelength light source. Scanning applications require quite demanding alignment tolerances between the different light emitters and since only two of these light sources could be fabricated in compatible material systems, we used a combination of hybrid and monolithic integration. Our device therefore consists of a monolithically integrated red/infrared (IR) dual-beam laser flipchip-bonded on a blue LED. The former are fabricated side by side with 50-μm spacing by selective etch of the red and regrowth of the IR laser structure [4]. A PbSn-solder-based flipchip bonding process [5] was used to package these red/IR lasers on top of a blue LED [6]. The vertical gap between blue and red/IR devices was on the order of 35 μm and in the lateral direction and the blue light emitter was placed exactly in the center between the two other lasers.

The authors are with the Xerox Palo Alto Research Center, Palo Alto, CA 94304 USA.

II. Fabrication Technology

In this paragraph, we describe first the fabrication of the red/IR lasers and the blue LED's [7]. We will then give some processing details about the additional fabrication steps necessary to prepare the flipchip bonding.

Monolithically integrated red/IR lasers were fabricated side-by-side with a photolithographically defined spacing of exactly 50 μm as described elsewhere [4]. The fabrication relied on MOCVD-type epitaxial growth of a full-red laser structure consisting of 750-nm-thick AlInP cladding layers, a 250-nm-thick $(Al_{0.4}Ga_{0.6})_{0.5}In_{0.5}P$ waveguide and an 8-nm-thick $Ga_{0.4}In_{0.6}P$ QW. On top of this structure, we grew a 100-nm-thick highly p-doped GaAs contact layer. We then etched this red laser structure back to the substrate using a Si_3N_4 etch mask and wet etch chemistry. After etching, the wafer was taken back to the growth reactor for deposition of a full-IR laser structure, consisting of 750-nm-thick AlInP cladding layers and a 250-nm-thick AlGaAs waveguide and a 9-nm-thick GaAs QW. Standard procedures [8] were used to fabricate 4-μm-wide metal clad ridge waveguide lasers. The two devices were thermally and electrically isolated by a 2-μm-deep isolation trench. Finally, electrical contacts were added.

For the InGaN–GaN-based blue LED, we first deposited the epitaxial layers on a C-face sapphire substrate using metal–organic chemical vapor disposition (MOCVD). The layer structure consisted of an active layer with ten 3-nm-thick $In_{0.2}Ga_{0.8}N$ QW's separated by 5-nm-thick GaN barriers which were embedded between two 100-nm-thick GaN confinement layers. Two 500-nm-thick $Al_{0.07}Ga_{0.93}N$ cladding layers on each side were employed to give sufficient optical confinement. These layers were grown on top of a 4-μm-thick GaN layer and covered with a 100-nm-thick GaN contact layer. Ridge waveguide LED's were then formed using chemically assisted ion beam etching (CAIBE) and CAIBE-etched mesas enabled lateral n-contacting. As shown in the schematic top view of the device (Fig. 1), there were also two additional metal pads on each side of the LED in addition to its p- and n-contacts. These were used as contact wires for the red/IR p-contacts, which were connected by the flipchip bonding process.

Preparation for the flipchip bonding was then exactly the same for both red/IR and blue light emitters. It started with

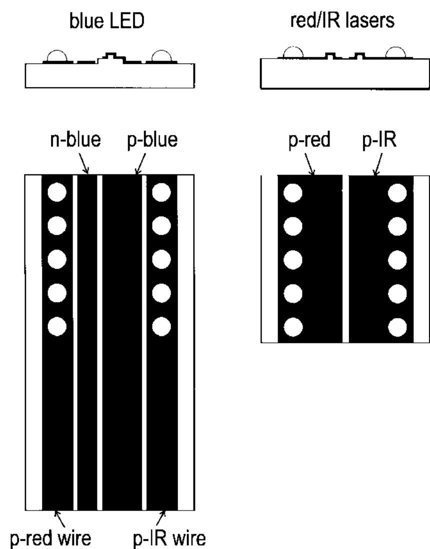

Fig. 1. Schematic drawing of the metal layers and wettable metal pads on a blue LED substrate piece and the red/IR laser device.

the deposition of a SiON layer on top of the existing devices. Circular holes with a diameter of 50, 70, or 90 μm were then etched into the SiON layer in order to define circularly shaped wettable metal pads for the PbSn solder. As shown in Fig. 1, five 50-μm holes (or three 70-μm holes or two 90-μm holes) fitted onto each wiring contact pad of the GaN LED. On top of these layers, we liftoff deposited Pb and Sn in a 60%–40% weight ratio and to a final thickness of 10 μm. The diameters of the PbSn disks on top of the 50-, 70-, and 90-μm holes were 55, 110, and 160 μm, respectively. The larger diameters of the solder disks account for the fact that we had to deposit the appropriate amount of metal for the formation of hemispheres in all three cases. After a reflow at 200 °C using soldering flux, we ended up with exactly hemispherically shaped solder-bumps. Next, we cleaved the red/IR lasers into 500 × 500 μm^2 pieces, and the blue LED's into sawed/polished bars of 1-mm width and 10-mm length. By using a commercial flipchip aligner/bonder, we then aligned the red/IR devices on top of the blue LED's. Tacky soldering flux was used to hold the pieces in place when transferring them to a hotplate. After the second reflow, which was carried out also at 200 °C, we cleaned the devices from flux remnants by using flux remover. As shown in the SEM picture of Fig. 2, a wire bond was then made to connect the n-contact of the red/IR devices with the n-contact of the blue LED.

III. Experimental Results

With the process described in the former paragraph, we could fulfill tight alignment tolerances of ±2 μm. This becomes obvious when looking at the SEM photograph of Fig. 3, where the ridge waveguide of the blue LED aligns very well with the isolation trench in the center between the red/IR lasers. In the vertical direction, the gap was on the order of 35 μm, depending on how much solder was evaporated initially.

Electrooptical testing of the red/IR lasers was done at room temperature and at continuous-wave (CW) conditions. The sapphire substrate of the blue LED, which was operated pulsed only, served as a heat-sink for the flipchip-bonded lasers. As shown in Fig. 4, we observed threshold currents of 12/41 mA

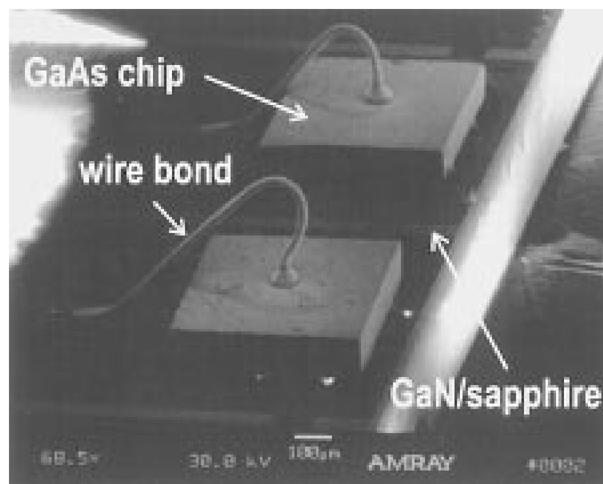

Fig. 2. SEM picture showing two flipchip-bonded GaAs-based red/IR lasers on an InGaN–GaN-based blue LED. The wire bonds connect the n-contacts of all three devices.

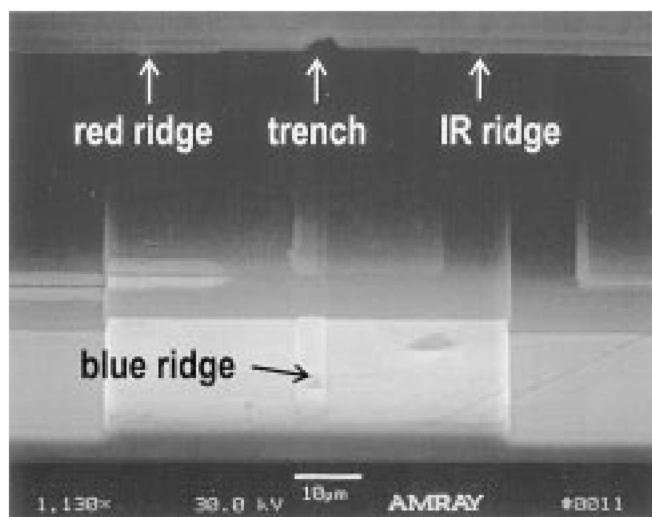

Fig. 3. SEM picture showing the precise alignment between the red/IR laser piece and the sapphire substrate with a blue LED.

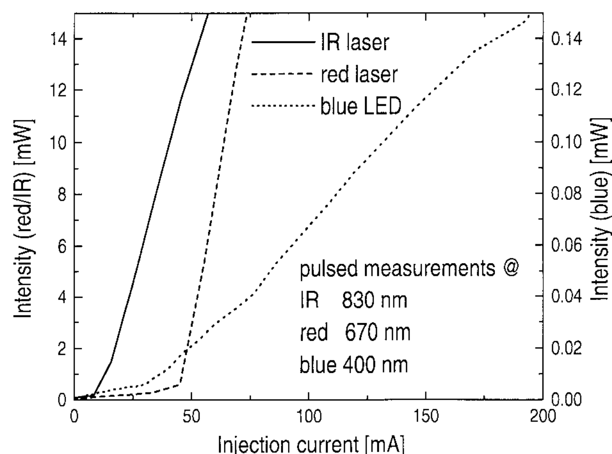

Fig. 4. L–I-curves of the red/IR lasers and the blue LED.

and slope efficiencies of 0.625/0.8 W/A for the IR/red devices, respectively. The blue LED emitted up to 500-μW pulsed optical power at typical current levels of 300 mA. In order to characterize the heat-sinking behavior of the flipchip-bonded devices, we compared their emission wavelengths for pulsed and CW operation, before and after bonding. The fact that we see comparable wavelength shifts before and after bonding between pulsed and CW operation indicates that p-sided heat-sinking via PbSn solder bumps and the sapphire substrate is efficient enough for our relatively moderate power levels. The emission wavelengths for pulsed/CW operated IR lasers were 824/832.9 nm for unbonded IR lasers and 823/829.6 nm for bonded IR lasers. Similarly, we observed emission wavelengths of 677.4/682.3 nm for unbonded red lasers and 675/680.3 nm for bonded red lasers. Again the numbers are measured for pulsed/CW operation. Thermal conductivity coefficients [9] are similar for GaAs (56 W/m·K) and GaN (65.6 W/m·K), and also reasonably high for PbSn solder (42 W/m·K). The coefficient for sapphire is the same order of magnitude; however there is decreasing heat conductivity at elevated temperatures (46 W/m·K at room temperature and 25 W/m·K at 100 °C). But since the operating voltages of the red/IR devices were relatively low, no big heating effects were seen even under CW operation. The emission wavelength of the blue LED's was on the order of 420 nm.

IV. Reliability Considerations

Although one is, in general, concerned about temperature cycles when doing flipchip soldering joints, these problems do not necessarily apply to the devices described here. There are some device-specific reasons for that. The most important one is probably that the thermal expansion coefficients of sapphire (5.4×10^{-6} K^{-1}) and GaAs (5.7×10^{-6} K^{-1}) are very similar. The second reason is the size of the laser chips. While the common fatigue considerations apply especially to chip sizes on the order of millimeters or even larger, our bonding area covers only 500×500 μm^2. Assuming a maximal distance of a solder bump joint from the chip center of 500 μm, we end up with a relative length difference of only 0.3 μm for 200 K temperature increase. As outlined in the previous paragraph, such a big temperature increase is not very likely for normal operating conditions of these lasers.

V. Conclusion

We presented a multiwavelength light emitter consisting of monolithically integrated red/IR lasers flipchip-bonded on top of a blue GaN-based LED. The red/IR lasers could be operated under CW conditions without detrimental device heating due to a lack of heat-sinking. We believe that this device architecture has the potential to impact color scanning systems. The flipchip process used in this work was based on PbSn solder which was deposited by a liftoff evaporation technique. Since all relevant process relied on photolithography, a very tight alignment tolerance of ± 2 μm in the lateral direction could be achieved.

Acknowledgment

The authors are grateful to D. A. Horine, P. Floyd, D. P. Bour, and R. Bringans for helpful discussions and R. Donaldson and E. Taggart for technical assistance.

References

[1] D. Hofstetter, H. P. Zappe, J. E. Epler, and P. Riel, "Multiple wavelength Fabry–Perot lasers fabricated by vacancy-enhanced quantum well disordering," *Appl. Phys. Lett.,* vol. 67, no. 14. pp. 1978–1980, 1995.

[2] D. P. Bour, D. W. Treat, K. Beernink, and R. L. Thornton, "Infra-red AlGaAs and visible AlGaInP laser-diode stack," *Electron. Lett.,* vol. 29, no. 21, pp. 1855–1856, 1993.

[3] Y. Qian, Z. H. Zhu, Y. H. Lo, H. Q. Hou, M. C. Wang, and W. Lin, "1.3 μm vertical-cavity surface-emitting lasers with double bonded GaAs/AIA's Bragg reflectors," *IEEE Photon. Technol. Lett.,* vol. 9, pp. 8–10, Jan. 1997.

[4] D. Sun, D. W. Treat, K. Beernink, R. D. Bringans, and G. J. Kovacs, "Red and infrared side by side semiconductor quantum well lasers integrated on GaAs substrate," *Appl. Phys. Lett.,* to be published.

[5] J. F. Kuhmann and D. Pech, "*In situ* observation of the self-alignment during FC-bonding under vacuum with and without H2," *IEEE Photon. Technol. Lett.,* vol. 8, pp. 1665–1667, Dec. 1996.

[6] L. F. Miller, "Controlled collapse chip-joining," *IBM J. Res. Dev.,* pp. 239–250, May 1969.

[7] M. Kneissl, D. P. Bour, L. T. Romano, C. Dunnrowicz, R. M. Donaldson, B. S. Krusor, and N. M. Johnson, *Appl. Phys. Lett.,* vol. 72, no. 14, pp. 700–702, 1998.

[8] D. P. Bour, R. S. Geels, D. W. Treat, T. L. Paoli, F. A. Ponce, R. L. Thornton, B. S. Krusor, R. D. Bringans, and D. F. Welch, "Strained $Ga_xIn_{l-x}P/(AlGa)_{0.5}P$ heterostructures and quantum well laser diodes," *IEEE J. Quantum Electron.,* vol. 30, pp. 593–607, Feb. 1994.

[9] *CRC Handbook of Chemistry and Physics,* 78th ed., 1987.